Mendeleev Communications

*Mendeleev Commun.*, 2025, **35**, 217–220

# Molecular structure of gaseous 1,1′,2,2′-tetramethyl-3,3′-bidiaziridine, established by electron diffraction and quantum chemical calculations

**Alexander V. Belyakov,[a] Vladimir V. Kuznetsov,[b] Galina S. Shimanskaya,[a] Anatoly N. Rykov,[c] Andrey S. Dmitrenok,[b] Dmitry V. Khakimov,[b] Konstantin L. Tokarev*[c] and Igor F. Shishkov*[c]**

[a] *St. Petersburg State Institute of Technology (Technical University), 190013 St. Petersburg, Russian Federation*
[b] *N. D. Zelinsky Institute of Organic Chemistry, Russian Academy of Sciences, 119991 Moscow, Russian Federation*
[c] *Department of Chemistry, M. V. Lomonosov Moscow State University, 119991 Moscow, Russian Federation. E-mail: igormg@mail.ru; annulen@yandex.ru*

DOI: 10.71267/mencom.7593

**The equilibrium geometry of the 1,1′,2,2′-tetramethyl-3,3′-bidiaziridine (TMBDA) molecule in the gas phase was determined using the gas-phase electron diffraction method in combination with quantum chemical calculations up to the all-electron RI-MP2/def2-QZVPP level of theory. It was confirmed that the TMBDA conformer with $C_2$ symmetry dominates in the gas phase. Quantum chemical simulations of the crystal packing of TMBDA showed that the racemic form has lower lattice energy than the *meso*-form, which is consistent with the experimental ratio in the synthesized product.**

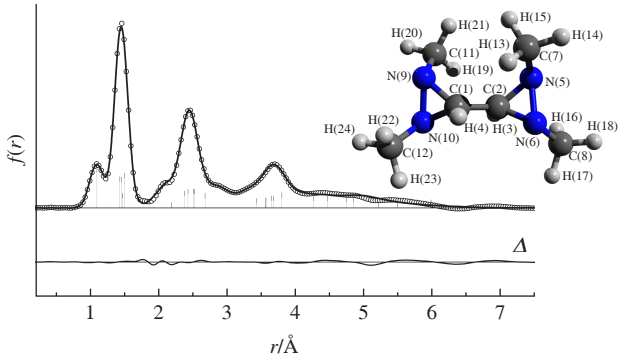


*Keywords*: diaziridines, synthesis, molecular structure, gas electron diffraction, quantum chemical calculations.

Structural analysis of molecules containing a diaziridine ring, although it has a long history, still remains relevant.[1–4] This is explained by the high applied and theoretical significance of these compounds. Thus, a number of known diaziridine derivatives have pronounced neurotropic activity.[5,6] Some representatives of this class of compounds are supposed to be used as low-toxic components of combustible mixtures in rocket engines instead of toxic hydrazine derivatives.[7,8] Diaziridine derivatives have found wide application as synthons for the preparation of various five- to eight-membered heterocyclic molecules.[9] These compounds turned out to be convenient objects for studying the stereochemistry of the nitrogen atom.[5,8]

In this communication, we report the synthesis of 1,1′,2,2′-tetramethyl-3,3′-bidiaziridine (TMBDA) **1** and our experimental and theoretical results of investigating possible stereocenter configurations and structural parameters of its molecule (Figure 1) using gas-phase electron diffraction (GED), spectral analysis and quantum chemical calculations.

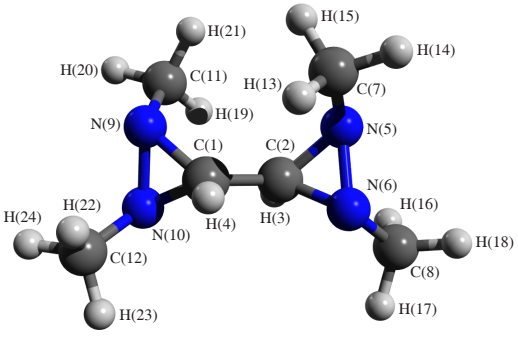


**Figure 1** Ball-and-stick model of the TMBDA molecule of $C_2$ symmetry with atom numbering.

The first mention of TMBDA and its physicochemical properties such as mp –7 °C, bp 156 °C (760 Torr) and $d_{exp}$ 0.957 g cm$^{-3}$ (20 °C) dates back to 1994.[10] However, its synthesis procedure and stereochemistry were first published only ten years later.[11] According to NMR spectroscopy data,[11] TMBDA is obtained as a mixture of racemate **1a** and *meso*-form **1b** in a ratio of 3 : 2 (Figure S1.1, see Online Supplementary Materials). Upon cooling the resulting diastereomer mixture to –18 °C, a crystalline product was isolated, which, according to X-ray diffraction analysis, turned out to be *meso*-form **1b** with mp 40 °C and $d_{calc}$ 1.066 g cm$^{-3}$.[11]

In this work, we synthesized TMBDA in a single step from methylamine, glyoxal and *tert*-butyl hypochlorite in methanol in 32.4% yield (for details, see Scheme S1.1 in Online Supplementary Materials), which is a significant improvement over the previously published synthesis scheme.[11] The implemented method is based on our previously developed approach to the synthesis of 1,2,3-trialkyldiaziridines, which consists of preliminary halogenation of excess aliphatic amine followed by introduction of a carbonyl compound into the reaction mixture.[12] Previously unknown 1,1′,2,2′-tetraethyl-3,3′-bidiaziridine (TEBDA) **2** and 1,1′,2,2′-tetrapropyl-3,3′-bidiaziridine (TPBDA) **3** were also prepared according to this scheme using ethylamine and propylamine, respectively.

Column chromatography was used to isolate products **1**–**3**. During the isolation of TMBDA, the racemate/*meso*-form ratio in the first (10%), main (80%) and final (10%) fractions of the isolated product **1** according to the $^1$H NMR spectrum was 67 : 33, 53 : 47 and 48 : 52, respectively. After vacuum distillation of the

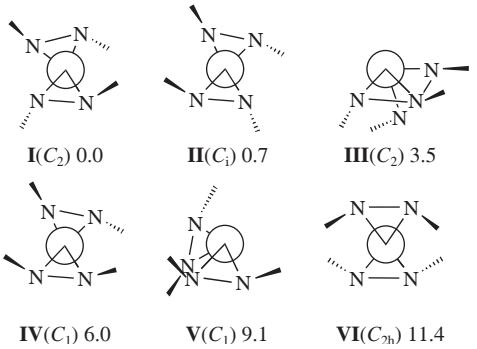


**Figure 2** Newman projections and relative Gibbs energies (kcal mol$^{-1}$) of TMBDA conformers at the B3LYP/6-311++G** level of theory.

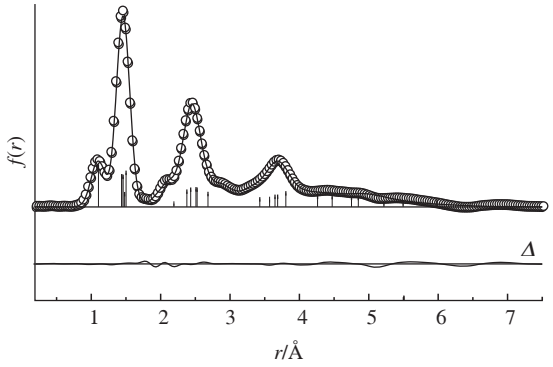


**Figure 3** Experimental (○) and calculated (—) radial distribution functions $f(r)$ of TMBDA and their difference ($\Delta$) estimated by subtracting the theoretical values from the experimental ones.

isolated product **1**, the fraction with bp 68–70 °C (18 Torr) was characterized by the racemate/*meso*-form ratio of 66 : 34. This product was used in the GED experiments.

The structure of a single TMBDA molecule in the gas phase was determined from a combination of GED data (for the procedure and experimental setup, see Section S3 and Table S3.1, respectively, in Online Supplementary Materials) and quantum chemical calculations. Geometry optimization runs were performed at the level of the all-electron second-order Møller–Plesset perturbation theory in the resolution-of-identity approximation (RI-MP2)[13] using the def2-QZVPP basis set[14] and at the level of density functional theory (DFT) with the B3LYP hybrid exchange-correlation functional[15,16] using the cc-pVTZ[17] basis set. The calculations were performed using the ORCA 4.2.0[18] and Gaussian 16 (Rev. C.01)[19] software packages, respectively. The resulting relative total electron energies of the structures found at the DFT level are shown next to the structures in Figure 2.

Normal coordinate analysis confirmed that the structures correspond to minima of the potential energy surface (PES). The mean amplitudes ($u_{ij,h1}$) and vibrational corrections ($r_{ij,e} - r_{ij,a}$) required for the GED data analysis (Table S4.4) were calculated using quadratic and cubic force fields within the first-order perturbation theory taking into account nonlinear kinematic effects using the SHRINK program.[20–23] The quadratic and cubic force fields were calculated using the B3LYP functional and the cc-pVTZ basis set.

Least-squares structure refinements were performed using a modified version of the KCED25 program.[24] The weight matrices were diagonal. The GED camera distance data were taken with weights of 0.5 and 1.0 for the short and long camera distances, respectively.

The molecular structure of TMBDA with $C_2$ symmetry (see Figure 1) is determined by seven bond distances C(1)–C(2), C(2)–N(5), C(2)–N(6), N(5)–C(7), N(6)–C(8), N(5)–N(6) and C–$H_{av}$; three nonbonding distances C(1)···N(5), N(5)···H(3) and C(1)···N(6); nine bond angles C(1)–C(2)–H(3), C(2)–N(5)–C(7), C(2)–N(6)–C(8), N(5)–C(7)–H(13), N(5)–C(7)–H(14), N(5)–C(7)–H(15), N(6)–C(8)–H(16), N(6)–C(8)–H(17) and N(6)–C(8)–H(18); and nine dihedral angles H(3)–C(2)–C(1)–H(4), H(3)–C(2)–N(5)–C(7), H(3)–C(2)–N(6)–C(8), C(2)–N(5)–C(7)–H(13), H(13)···N(5)–C(7)–H(14), H(13)···N(5)–C(7)–H(15), C(2)–N(6)–C(8)–H(16), H(16)···N(6)–C(8)–H(17) and H(16)···N(6)–C(8)–H(18). Starting from the theoretical MP2 and DFT values, the geometric parameters and the mean least-squares vibrational amplitudes were refined in groups with constant differences. The mean least-squares amplitudes were refined in seven groups based on the specified ranges of the radial distribution curve (Figure 3): 1.0–1.3, 1.3–1.8, 1.8–3.1, 3.1–4.1, 4.1–5.2, 5.2–6.5 and 6.4–8.0 Å. The internuclear distances were refined in three groups: the C–$H_{av}$ bond distance, all other bond distances and the C(1)···N(5) and C(1)···N(6) distances. The C(2)–N(5)–C(7) and C(2)–N(6)–C(8) bond angles were refined in a group, the remaining bond and dihedral angles were set equal to the theoretical MP2 values. The resulting structural parameters for the lowest-energy molecular model of $C_2$ symmetry are listed in Table 1.

The lowest torsional vibration frequency in the TMBDA molecule, about 40 cm$^{-1}$, is related to vibrations around the central C(1)–C(2) bond. The percentage of the second conformer of the $C_i$ symmetry could not be determined due to the weak contribution from the methyl groups of different rings and the large amplitude of vibrations around the central C(1)–C(2) bond.

To evaluate the thermochemical properties of the compounds, as well as to explain the higher proportion of *meso*-form **1b** in the synthesized product compared to racemate **1a**, we calculated their enthalpies of formation in the gas and solid phases, as well as the enthalpies of combustion. It was interesting to compare the obtained values with those of all-hydrocarbon analogs **4a**,**b**, so we modeled the crystal packings for them as well.

Quantum chemical modeling of crystal packings was carried out in the 'blind test' paradigm without using experimental data

**Table 1** Main equilibrium structural parameters of the TMBDA molecule of $C_2$ symmetry.[a]

| Parameters | GED | MP2/QTZ | B3LYP/VTZ |
|---|---|---|---|
| | Internuclear distances/Å | | |
| C(1)–C(2) | 1.476(16) | 1.489 | 1.498 |
| C(2)–N(5) | 1.439(16) | 1.451 | 1.449 |
| C(2)–N(6) | 1.431(16) | 1.443 | 1.442 |
| N(5)–N(6) | 1.469(16) | 1.482 | 1.477 |
| N(5)–C(7) | 1.447(16) | 1.460 | 1.462 |
| N(6)–C(8) | 1.445(16) | 1.458 | 1.461 |
| $(C–H)_{av}$ | 1.084(7) | 1.088 | 1.092 |
| C(1)···N(5) | 2.552(23) | 2.576 | 2.599 |
| C(1)···N(6) | 2.469(23) | 2.493 | 2.507 |
| N(5)···H(3) | 2.130[b] | 2.130 | 2.127 |
| | Bond angles/deg | | |
| C(1)–C(2)–H(3) | 115.0[b] | 115.0 | 114.0 |
| C(2)–N(5)–C(7) | 115.0(2.1) | 116.0 | 118.6 |
| C(2)–N(6)–C(8) | 112.6(2.1) | 113.6 | 115.7 |
| | Dihedral angles/deg | | |
| H(3)–C(2)–N(5)–C(7) | 151.3[b] | 151.3 | 150.0 |
| H(3)–C(2)–N(6)–C(8) | 4.0[b] | 4.0 | 2.3 |
| H(3)–C(2)–C(1)–H(4) | 148.8[b] | 148.8 | 158.1 |

[a] *R*-factor is 7.5%. Values in parentheses are 3$\sigma$ standard deviations of the least squares refinement. Atom numbering is shown in Figure 1. Parameters with the same least squares errors were combined into one group with differences fixed at the quantum chemical values. [b] Parameters were fixed at the quantum chemical values.

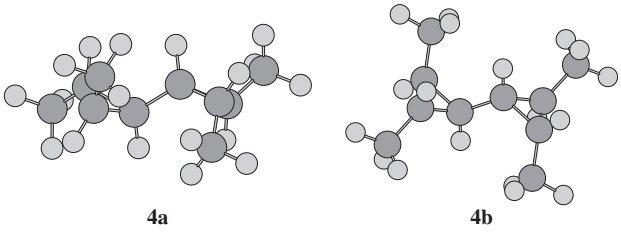


**Figure 4** All-hydrocarbon analogs of TMBDA: racemate **4a** and *meso*-form **4b**.

input. To search for global minima on the PES, when optimizing the geometry of molecules **1a**,**b** (see Figure S1.1) and **4a**,**b** (Figure 4), the DFT method with the B3LYP functional and the aug-cc-pVDZ basis set[17,25] with the Grimme dispersion correction DFT-D2[26] was used. All molecular structure calculations were performed using the Gaussian 09 (Rev. D.01) program.[19] The resulting molecular structures were subsequently considered rigid and were used as starting models when constructing the initial crystal lattices for their subsequent optimization. To model the crystal structure, the method of atom–atom potentials was used, where the energy of the crystal lattice ($U_{latt}$) was represented as the sum of van der Waals interactions ($U_{vdw}$) and electrostatic interactions ($U_{coul}$): $U_{latt} = U_{vdw} + U_{coul}$, *i.e.*, the optimal crystal packing was found by optimizing the parameters of the unit cell of the crystal and localizing the minima on the corresponding PES. The van der Waals interactions were represented as a Lennard–Jones '6–12' potential,[27] and the electrostatic energy was calculated for molecular models in which point charges were optimized by the FitMEP program taking into account both the magnitude of the charges and the positions of their centers so that these charges most accurately describe the molecular electrostatic potential.[28] A set of starting crystal lattice models with certain positions of molecules in it and subsequent PES scanning were carried out using the current version of the PMC software package.[29]

An extended list of the most common space groups was selected, including $P2_1/c$, $P2_12_12_1$, $P\bar{1}$, $P2_1$, $Pbca$, $C2/c$, $Pna2_1$, $Pnma$, $Pca2_1$, $Cc$, $C2$, $P1$, $P2_1/m$, $Pbcn$, $Pc$, $P4_12_12$, $P4_1$, $Pccn$, $Fdd2$, $Cmc2_1$, $P3_1$, $R\bar{3}$, $P2_12_12$, $I4_1/a$, $P6_1$, $P42/n$, $Pbcm$, $C2/m$, $Pmn2_1$, $Iba2$, $P\bar{4}2_1c$, $R3$, $P3_12_1$, $P2/c$ and $C222_1$, since these 35 space groups cover 97% of all experimental crystal structures studied.[30] Packings with one ($Z' = 1$) and two ($Z' = 2$) independent molecules in a unit cell are considered.

Crystal packings were calculated according to the scheme described earlier.[31,32] The G3B3 method[33] was used to estimate the enthalpies of formation in the gas phase. The enthalpies of sublimation were calculated using the formula $H_L = -E_{latt} - 2RT$, where $E_{latt}$ is the lattice energy, $R$ is the universal gas constant, and $T$ is the temperature (298 K). The modeling yielded crystal packings for *meso*-form **1b** (Table S5.3) and racemic form **1a** (Table S5.4) of TMBDA. Table S5.3 also provides the parameters of the experimentally determined structure CCDC 260030.[34]

To adjust densities to different temperatures, it is necessary to know the coefficients of thermal expansion, which in general can be highly nonlinear or even negative, but volumetric coefficients are usually in the range of $(1.3–2.5)\times10^{-4}$ K$^{-1}$.[35] For this reason, we present a range of predicted densities for model packings.

The main parameters in assessing crystal packings are the relative arrangement of molecules in the unit cell, the density and the lattice energy, while the true space group may be a subgroup of the model or may be somewhat inaccurate due to differences in lattice parameters.

Comparison of the resulting packings showed that the 3rd model polymorph coincides with the experimental packing (Figure S5.1). In the model, the lattice parameters were obtained for the alternative group $P2_1/n$, and for clarity of comparison we further reduced the lattice parameters to $P2_1/c$. The estimated density for the model is quite close to the experimental value.

Initially, the stereochemistry of the molecule was assumed to be unknown, and we simulated crystals for both forms. It can be seen that the density and lattice energy of the racemic form are lower than those of the *meso*-form.

**Table 2** Thermochemical properties of TMBDA stereoisomers **1a**,**b** and their hydrocarbon analogues **4a**,**b**.

| Compound | $\Delta H_f^0$(g.)/ kJ mol$^{-1}$ | $\Delta H_{subl}$/ kJ mol$^{-1}$ | $\Delta H_f^0$(s.)/ kJ mol$^{-1}$ | $-\Delta H_{comb}$/ kJ mol$^{-1}$ | $\Delta H_{comb}$/ MJ kg$^{-1}$ |
|---|---|---|---|---|---|
| **1a** | 448.99 | 75.21 | 373.38 | 1131.9 | 33.3 |
| **1b** | 444.41 | 65.88 | 378.52 | 1133.0 | 33.4 |
| **4a** | 26.4 | 69.98 | –43.59 | 1544.9 | 46.8 |
| **4b** | 25.58 | 64.25 | –38.67 | 1546.1 | 46.8 |

Table 2 shows the calculated enthalpies of formation in the solid state $\Delta H_f^0$(s.) and lower enthalpies of combustion $\Delta H_{comb}$ for compounds **1a**,**b** and hydrocarbon compounds **4a**,**b** similar in structure.

When calculating the enthalpy of sublimation of *meso*-form **1b**, we took the lattice energy of the polymorph that coincides with the experiment; however, even if we consider the first polymorph in terms of energy, the difference is only 0.16 kcal mol$^{-1}$, which will not introduce a significant error in calculating the enthalpy of combustion. The enthalpy of formation of *meso*-form **1b** in terms of lattice energy and the enthalpy of formation in the solid state is lower than that of racemic form **1a**, which indicates its higher thermodynamic stability and additionally confirms the experimentally established structure of *meso*-form **1b**. For example, the lowest enthalpy of combustion for kerosene is about 43 MJ kg$^{-1}$. Thus, hypothetical fuel based on compounds **4a** or **4b** could have increased heat release values at the level of propane or ethane (46–47 MJ kg$^{-1}$), but be in a condensed state.

A.N.R., K.L.T. and I.F.Sh. acknowledge that this work was carried out within the framework of the state assignment of the Russian Federation 'Molecular and supramolecular organization of compounds, hybrid and functional materials' (contract no. 121031300090-2).

*Online Supplementary Materials*

Supplementary data associated with this article can be found in the online version at doi: 10.71267/mencom.7593.

## References

1 V. V. Kuznetsov, N. N. Makhova and M. O. Dekaprilevich, *Russ. Chem. Bull.*, 1999, **48**, 617; https://doi.org/10.1007/bf02496194.
2 A. V. Belyakov, V. V. Kuznetsov, G. S. Shimanskaya, A. N. Rykov, A. S. Goloveshkin, Y. V. Novakovskaya and I. F. Shishkov, *Mendeleev Commun.*, 2023, **33**, 95; https://doi.org/10.1016/j.mencom.2023.01.030.
3 A. V. Belyakov, V. V. Kuznetsov, N. S. Kormil'tsina, G. S. Shimanskaya, A. N. Rykov, A. S. Dmitrenok, Y. V. Novakovskaya and I. F. Shishkov, *Mendeleev Commun.*, 2023, **33**, 653; https://doi.org/10.1016/j.mencom.2023.09.021.
4 I. I. Marochkin, P. Yu. Sharanov, V. V. Kuznetsov, I. F. Shishkov and Y. V. Novakovskaya, *Mendeleev Commun.*, 2024, **34**, 543; https://doi.org/10.1016/j.mencom.2024.06.024.
5 M. Kamuf and O. Trapp, *Chirality*, 2011, **23**, 113; https://doi.org/10.1002/chir.20885.
6 N. N. Makhova, V. Y. Petukhova, A. V. Shevtsov, V. V. Novakovskiy and V. V. Kuznetsov, *Patent WO 2013/111118 A3*, 2013; https://patentimages.storage.googleapis.com/2d/0b/ad/c5366c732821ea/WO2013111118A3.pdf.
7 X. Zhang, L. Shen, Y. Luo, R. Jiang, H. Sun, J. Liu, T. Fang, H. Fan and Z. Liu, *Ind. Eng. Chem. Res.*, 2017, **56**, 2883; http://doi.org/10.1021/acs.iecr.6b04842.

8 V. V. Kuznetsov, D. V. Khakimov, A. I. Samigullina and A. S. Dmitrenok, *Chem. Phys.*, 2024, **579**, 112187; https://doi.org/10.1016/j.chemphys.2024.112187.

9 N. N. Makhova, L. I. Belen'kii, G A. Gazieva, I. L. Dalinger, L. S. Konstantinova, V. V. Kuznetsov, A. N. Kravchenko, M. M. Krayushkin, O. A. Rakitin, A. M. Starosotnikov, L. L. Fershtat, S. A. Shevelev, V. Z. Shirinian and V. N. Yarovenko, *Russ. Chem. Rev.*, 2020, **89**, 55; https://doi.org/10.1070/rcr4914.

10 E. Ya. Zandberg, A. L. Nezdyurov, V. I. Paleev, G. A. Goryunova and L. N. Chudakov, *Russ. J. Org. Chem.*, 1994, **30**, 524.

11 V. Yu. Petukhova, N. N. Makhova, V. P. Ananikov, Yu. A. Strelenko and I. V. Fedyanin, *Russ. Chem. Bull.*, 2004, **53**, 641; https://doi.org/10.1023/B:RUCB.0000035650.08227.36.

12 V. V. Kuznetsov, V. V. Seregin, D. V. Khakimov, T. S. Pivina, M. D. Vedenyapina, A. A. Vedenyapin and N. N. Makhova, *Russ. Chem. Bull.*, 2014, **63**, 2000; https://doi.org/10.1007/s11172-014-0691-7.

13 M. Feyereisen, G. Fitzgerald and A. Komornicki, *Chem. Phys. Lett.*, 1993, **208**, 359; https://doi.org/10.1016/0009-2614(93)87156-W.

14 F. Weigend, F. Furche and R. Ahlrichs, *J. Chem. Phys.*, 2003, **119**, 12753; https://doi.org/10.1063/1.1627293.

15 A. D. Becke, *J. Chem. Phys.*, 1993, **98,** 5648; https://doi.org/10.1063/1.464913.

16 P. J. Stephens, F. J. Devlin, C. F. Chabalowski and M. J. Frisch, *J. Phys. Chem.*, 1994, **98**, 11623; https://doi.org/10.1021/j100096a001.

17 T. H. Dunning, Jr., *J. Chem. Phys.*, 1989, **90**, 1007; https://doi.org/10.1063/1.456153.

18 F. Neese, *Wiley Interdiscip. Rev.: Comput. Mol. Sci.*, 2018, **8**, e1327; https://doi.org/10.1002/wcms.1327.

19 M. J. Frisch, G. W. Trucks, H. B. Schlegel, G. E. Scuseria, M. A. Robb, J. R. Cheeseman, G. Scalmani, V. Barone, G. A. Petersson, H. Nakatsuji, X. Li, M. Caricato, A. V. Marenich, J. Bloino, B. G. Janesko, R. Gomperts, B. Mennucci, H. P. Hratchian, J. V. Ortiz, A. F. Izmaylov, J. L. Sonnenberg, D. Williams-Young, F. Ding, F. Lipparini, F. Egidi, J. Goings, B. Peng, A. Petrone, T. Henderson, D. Ranasinghe, V. G. Zakrzewski, J. Gao, N. Rega, G. Zheng, W. Liang, M. Hada, M. Ehara, K. Toyota, R. Fukuda, J. Hasegawa, M. Ishida, T. Nakajima, Y. Honda, O. Kitao, H. Nakai, T. Vreven, K. Throssell, J. A. Montgomery, Jr., J. E. Peralta, F. Ogliaro, M. J. Bearpark, J. J. Heyd, E. N. Brothers, K. N. Kudin, V. N. Staroverov, T. A. Keith, R. Kobayashi, J. Normand, K. Raghavachari, A. P. Rendell, J. C. Burant, S. S. Iyengar, J. Tomasi, M. Cossi, J. M. Millam, M. Klene, C. Adamo, R. Cammi, J. W. Ochterski, R. L. Martin, K. Morokuma, O. Farkas, J. B. Foresman and D. J. Fox, *Gaussian 16, Revision C.01*, Gaussian, Inc., Wallingford, CT, 2016; https://gaussian.com/gaussian16/.

20 V. A. Sipachev, *J. Mol. Struct.: THEOCHEM*, 1985, **121**, 143; https://doi.org/10.1016/0166-1280(85)80054-3.

21 V. A. Sipachev, in *Advances in Molecular Structure Research*, eds. M. Hargittai and I. Hargittai, JAI Press, New York, 1999, vol. 5, pp. 263–311; https://colab.ws/articles/10.1016/S1087-3295(99)80009-7.

22 V. A. Sipachev, *J. Mol. Struct.*, 2001, **567**–**568**, 67; https://doi.org/10.1016/S0022-2860(01)00534-8.

23 V. A. Sipachev, *Struct. Chem.*, 2000, **11**, 167; https://doi.org/10.1023/A:1009217826943.

24 B. Andersen, H. M. Seip, T. G. Strand and R. Stølevik, *Acta Chem. Scand.*, 1969, **23**, 3224; https://doi.org/10.3891/acta.chem.scand.23-3224.

25 R. A. Kendall, T. H. Dunning, Jr. and R. J. Harrison, *J. Chem. Phys.*, 1992, **96**, 6796; https://doi.org/10.1063/1.462569.

26 S. Grimme, *J. Comput. Chem.*, 2006, **27**, 1787; https://doi.org/10.1002/jcc.20495.

27 F. A. Momany, L. M. Carruthers, R. F. McGuire and H. A. Scheraga, *J. Phys. Chem.*, 1974, **78**, 1595; https://doi.org/10.1021/j100609a005.

28 A. V. Dzyabchenko, *Russ. J. Phys. Chem. A*, 2008, **82**, 758; https://doi.org/10.1134/S0036024408050129.

29 A. V. Dzyabchenko, *Russ. J. Phys. Chem. A*, 2008, **82**, 1663; https://doi.org/10.1134/S0036024408100075.

30 A. J. Cruz Cabeza, E. Pidcock, G. M. Day, W. D. S. Motherwell and W. Jones, *CrystEngComm*, 2007, **9**, 556; https://doi.org/10.1039/B702073B.

31 D. V. Khakimov, A. V. Dzyabchenko and T. S. Pivina, *Russ. Chem. Bull.*, 2020, **69**, 212; https://doi.org/10.1007/s11172-020-2748-0.

32 D. V. Khakimov, L. L. Fershtat, T. S. Pivina and N. N. Makhova, *J. Phys. Chem. A*, 2021, **125**, 3920; https://doi.org/10.1021/acs.jpca.1c02960.

33 A. G. Baboul, L. A. Curtiss, P. C. Redfern and K. Raghavachari, *J. Chem. Phys.*, 1999, **110**, 7650; https://doi.org/10.1063/1.478676.

34 *CODATA Key Values for Thermodynamics*, eds. J. D. Cox, D. D. Wagman and V. A. Medvedev, Hemisphere Publishing Corp., New York, 1989; https://www.codata.info/resources/databases/key1.html.

35 A. van der Lee and D. G. Dumitrescu, *Chem. Sci.*, 2021, **12**, 8537; https://doi.org/10.1039/D1SC01076J.


*Received: 13th August 2024; Com. 24/7593*